Journal of Plankton Research
December 2023, Volume 45, Issue 6, Pages 785-793
https://doi.org/10.1093/plankt/fbad039 https://archimer.ifremer.fr/doc/00861/97283/

Phytoplankton metabolism in a stratified nearshore ecosystem with recurrent harmful algal blooms (HABs)

Regaudie-de-Gioux Aurore [1, *], Latorre L [2], Basterretxea G [2]

[1] Dyneco-Pelagos, FRench Institute for Sea Research, Ifremer Dyneco-Pelagos , 1625 Route De Sainte Anne, Plouzané 29280, France
[2] Department of Marine Ecology, Imedea (UIB-CSIC) , Miquel Marques 21, Esporles, Balearic Islands 07190, Spain

* Corresponding author : Aurore Regaudie-de-Gioux, email address : aregaudi@ifremer.fr

Abstract :

The coastal ocean is experiencing changes in its physical and chemical properties that strongly affect planktonic metabolism assemblages and, in some cases, favor the occurrence of harmful algal blooms (HABs). Here we analyze the variations in phytoplankton biomass, gross and net primary production (NCP) as well as community respiration (CR) at two nearshore sampling sites (P1 and P2) located at a Mediterranean beach where high biomass HABs are recurrent. At P1, the most exposed site, phytoplankton chlorophyll was generally low, whereas dinoflagellates outbreaks of the genus Gymnodinium and Alexandrium were recurrent during summer at P2 spanning for 10–20 days. During bloom episodes, NCP increased up to 10-fold (>80 mmol O2 m−3 day−1). Contrastingly, variation in CR only reached an average of 1.8-fold the rates of non-bloom conditions. Remarkably, although the enhanced NCP:CR ratio suggests net autotrophic population growth, production per unit biomass at P1 and P2 was not significantly different. Our results indicate that although summer conditions favor the necessary primary production enhancement leading to HAB occurrences, the short-term dynamics driving high biomass episodes are not driven by metabolic variations but instead are governed by subtle accumulative processes of some flagellate species in the nutrient-rich nearshore environment.

Keywords : HABs, primaryproduction, respiration, nearshorewaters, MediterraneanSea

1. Introduction

Ongoing climate change effects in the Mediterranean Sea (MS) are more pronounced than global scale variations (Cramer et al., 2018). These changes include the warming of surface waters, including eventual heat waves, and increased water column stratification (Lejeusne et al., 2010; Coma et al., 2009). Coupled with the dramatically increasing population and urbanization of coastal areas, nitrogen cycle, and phosphorous cycles have been extensively modified in the coastal waters of the MS because of the abundant supply of land-derived nutrients (e.g. Powley et al., 2018). These impacts are expected to produce significant effects in nitrogen-deficient areas of the tropical and subtropical oceans which are acutely vulnerable to nitrogen pollution (Beman et al., 2005). The interplay between increasing temperature, stratification, nutrient-enriched surface, and submarine groundwater discharges (SGD) in nearshore waters, among other causes, produce environmental changes with far-reaching consequences in marine ecosystems. For example, the warming of coastal waters combined with nutrient enrichment can deeply affect marine phytoplankton communities, changing their size structure, phenology, abundance, species composition, and turnover rates. These structure and metabolic variations can eventually trigger deleterious effects such as eutrophication and/or the occurrence of Harmful Algal Blooms (HABs; Wells et al., 2015).

HABs produce severe consequences on the socio-economic services provided by marine ecosystems affecting the well-being of local communities (e.g. Anderson et al. 2002; Berdalet et al. 2016). Several complexities modulating HAB occurrences, such as the role of life cycle stages, the biochemical and physical interactions involved, or climate drivers remain to be unraveled (Gobler, 2020). While these responses are not universal, with many other factors influencing the outcome of HAB dynamics every year in each location, concern has been growing considering that physical, chemical, and biological conditions necessary for the development and persistence of HABs are increasing, therefore favoring their potential occurrence (Wells et al., 2020).

Harmful blooms ultimately result from positive imbalances between phytoplankton growth/accumulation and loss terms such as mortality (either by grazing or by infections), and/or advection (Garces, 1999; Irigoien et al., 2005). Unlike early spring blooms in open ocean waters which are commonly produced by fast-growing diatoms and subsequently controlled by zooplankton grazing (Ribera d'Alcalà et al., 2004; Donoso et al., 2017), nearshore summer booms in the MS are typically generated by dinoflagellates such as *Alexandrium*, *Gymnodinium*, *Prorocentrum* or *Dinophysis* which are scarcely predated (e.g. Bravo et al., 1990; Calbet et al., 2003; Delgado et al., 1990). In the MS, these organisms

proliferate in nearshore waters within embayments, harbors, or other coastal features where growth is unconstrained by the lack of nutrients, producing small and localized high biomass episodes, with magnitudes highly exceeding those of spring blooms (i.e. $>10^6$ cells L^{-1}). Notably, while summer temperatures that maximize phytoplankton metabolism create the potential for biomass accumulation, bloom-forming dinoflagellates are rather large and complex organisms that do not show particularly high growth rates compared with other phytoplankton groups such as cryptophytes, chrysophytes, or diatoms (Stolte and Garces, 2006). Subtle variations in dinoflagellate metabolism or slight changes in coastal hydrographic conditions may favor the accumulation of cells leading to the initiation of a HAB event.

Phytoplankton growth rates are a composite trait that emerges through the interaction of more fundamental traits relating to biomass-specific production, nutrient uptake, and metabolism setting the pace of plankton variations (Padfield, et al. 2016; Ward et al., 2017). Indeed, phytoplankton growth rates are dependent on two metabolic fluxes: photosynthesis and respiration (Raven and Geider, 1988). However, few studies provide experimental measurements of changes in phytoplankton metabolism during HAB episodes. Most available information on HAB dynamics relies on phytoplankton biomass monitoring (using chlorophyll concentration as a proxy), and/or cell abundance and identification reports. The present study aims to characterize the year-round variations of plankton metabolism in a nearshore location recurrently affected by HAB episodes and to elucidate their role in overall HAB dynamics.

2. Material and Methods

2.1. Study site and sample collection

The sampling study was carried out on Peguera Beach, located on the western coast of Majorca Island (Balearic Islands, Spain; Fig. 1). Peguera is an embayed urban beach surrounded by tourist hotels and restaurants. Blooms have been recurrently reported since the 1990s. Microalgal cells, generally flagellates, accumulate in the beach center and eastern boundary, which are more protected from swells, producing intense water discolorations (e.g. Basterretxea et al., 2005; 2011).

A total of 161 samplings were carried out in nearshore waters at Peguera from April 2017 to September 2019. During the winter, sampling was performed every 15 days (from November to February) whereas, during the rest of the year, sampling frequency was increased to once a week and to twice a week during summer when bloom events were most

likely to occur. We sampled surface water on two distinct points of this beach; one at the more exposed western boundary of the beach (P1) and, another on the eastern side, which is protected by a headland (P2; Fig. 1). At every sampling, surface seawater temperature was measured using a CastAway^{TM} CTD until September 2018, and a YSI30 conductivity and temperature meter thereafter. Solar radiation, wind direction and velocity were obtained from Palma Bay meteorological buoy located alongside Peguera Beach. Data were recorded every 10 min.

For each sampling station (P1 and P2), surface seawater was carefully sampled with a bucket and transferred to two 5L carboys. The sample in one of the carboys was used for microplankton identification, chl-*a* estimation, inorganic nutrient concentrations, and salinity (S). The second sample was dedicated to planktonic metabolism estimations. This sample was immediately protected with a dark screen to avoid exposure to solar irradiance before the incubation.

2.2. Nutrients

Nutrient subsamples were withdrawn from the 5L carboys. Triplicate 15 mL samples were filtered through GF/F filters, and preserved in polypropylene tubes at -20°C until their analysis in the laboratory. Concentrations of dissolved nitrate (NO_3^-) and nitrite (NO_2^-) were measured using a Skalar autoanalyzer using colorimetric techniques (Grasshoff et al., 1999). The accuracy of the analysis was established using Coastal Seawater Reference Material for Nutrients (MOOS-1, NRC-CNRC). For the present study, nitrite and nitrate were summed and presented as NOx.

2.3. Chlorophyll-a concentration and microphytoplankton community composition

Duplicate sub-samples of 200 mL were filtrated onto GF/F filters for the quantification of the total chlorophyll-*a* concentration (chl-*a*). The pigments were extracted in 10 mL 90% acetone (v/v) for at least 24 h in the dark at 4°C and quantified using a calibrated Turner Trilogy fluorimeter. A calibration factor obtained from a commercial chl-*a* standard (Sigma-Aldrich C5753) was used to calculate the final chl-*a*.

Analysis of microphytoplankton species composition was carried out only during the bloom season. 250 mL sub-samples were collected at P2 during bloom periods (18 samples in total) and fixed in Lugol's iodine and stored in the dark until analysis. The general procedure for identifying and quantifying phytoplankton involved sedimentation (24 h) of a subsample 100 ml Utermöhl settling chamber and subsequent counting of all cells using an inverted microscope.

2.4. Characterization of short-term outbreaks

Blooms in Mallorca are generally characterized by a period of increased phytoplankton biomass during the summer in which several outbreaks composed of one or two dominant dinoflagellate species dominate microphytoplankton assemblages (e.g. Basterretxea et al., 2007). For the present study, the characteristics of these bloom episodes were determined using a reference threshold for non-bloom conditions. Considering the lack of chlorophyll variation over the seasons at P1, we decided to estimate the reference threshold using the chlorophyll concentration at this location. Indeed, this threshold was defined as two standard deviations from the long-term average of the chl-*a* times series at P1 from May to September for the three years. The chl-*a* times series at P2 was first interpolated to obtain a 1-day temporal resolution. If interpolated chl-*a* magnitudes at P2 rose the reference threshold from May to September of that year and lasted at least 7 days, we defined this episode as a bloom. The first day of the episode is chosen as the bloom initiation date of each year and its termination date is when chl-*a* concentration drops below the reference threshold.

2.5. Plankton metabolism

Water for metabolism experiments was prefiltered with 100 µm mesh to remove large organisms and suspended particulate matter (SPM). We are aware that some micrograzers get past this mesh affecting both production and respiration estimates. However, larger cells, such as dinoflagellates, cryptophytes, and diatoms, are often observed in the nearshore (Basterretxea et al., 2018) and the use of a finer mesh (i.e. 50 µm) could remove some of these populations. Gross primary production (GPP), net community production (NCP), and community respiration (CR) were estimated to establish the planktonic community metabolism present at each sampling station. NCP and CR were estimated from changes in oxygen concentration over 24 h. Dissolved oxygen concentration was measured using the spectrophotometric Winkler approach which shows a standard deviation of 0.45 % for inter-repeatability and 0.73 % for reproducibility near 250 µmol L^{-1} (Labasque et al., 2004). Seven 120 mL opaque 'dark' and 7 transparent 'light' borosilicate bottles were carefully filled with the sampled water used for the planktonic metabolism for P1 and P2. Additionally, 6 replicates were immediately fixed for the measurement of the initial oxygen concentration. Incubations of the 7 'light' bottles were performed within a temperature-controlled incubator illuminated by artificial light (daylight T8 18W 865ErP; photosynthetically active radiation, PAR, intensity of 71.91 µmol photon m^{-2} s^{-1}) under a day-night cycle. Light hours ranged from 9 h (winter) to 15 h (summer). Incubations of the 7 'dark' bottles were performed under complete darkness for 24 h. Both incubations were performed at the *in situ* temperature. CR and NCP were calculated from changes in dissolved oxygen concentration after incubation of

samples under ‘dark’ and ‘light’ conditions, respectively, and GPP was calculated by solving the mass balance equation GPP = NCP + CR. Occasionally, metabolism experiments failed and yielded ‘negative’ planktonic CR (*i.e.* production of oxygen in the dark) or negative GPP (*i.e.* CR > GPP). These estimates were not considered here.

3. Results

3.1. Environmental conditions

The seasonal trend of sea surface temperature followed a similar pattern at both sampling sites (P1 and P2), with minimum temperatures in February (~15°C) and maximum values in July-August (30-31°C; Fig. 2 and Table 1). From May to October, the temperature at P2 slightly exceeds that at P1, the maximum difference being at the end of June (+1.8°C). Conversely, P2 was slightly colder from October to March (up to -0.3°C). At P2, salinity fluctuated between 34.9 and 38.2 and was generally lower than at P1 (range 37 to 38.2). Indeed, both sampling points episodically displayed dramatic salinity declines (i.e. 0.5 to 1.5) some of which were coincident with NOx enhancements suggesting the influence of nutrient-rich groundwater seeps. Nevertheless, NOx displayed a rather random behavior without significant differences between summer and winter. Even so, the observed concentrations (> 1 mmol m^{-3}) contrasted with offshore values in the MS where NOx in summer is found at undetectable concentrations (e.g. Pasqueron de Fommervault et al., 2015).

Mean NOx values at P1 and P2 were relatively low (i.e. 0.8 and 1.1 mmol m^{-3}, respectively) but showed higher values during the sampling period (>3 mmol m^{-3}) without displaying any seasonal trend. Both salinity and NOx were significantly lower and higher respectively at P2 (Friedman test, $p < 0.05$). However, nutrient variations were seemingly random, and a poor correlation was obtained between salinity and NOx ($r = 0.09$, $p = 0.277$) (Table 1, Fig. 2).

3.2. Phytoplankton biomass and species composition

Phytoplankton biomass, measured as chl-*a* concentration showed significant differences between P1 and P2 (Friedman test, $p < 0.01$) that were exacerbated during summer (0.47 ± 0.12 and 3.99 ± 0.54 mg m^{-3} at P1 and P2, respectively; Table 2 and Fig. 2d). At P1, chl-*a* concentration showed low variability and overall reduced values (mean = 0.45 ± 0.09 mg m^{-3}). Contrastingly, the overall biomass trend at P2 was defined by an exponential increase from late May to August, composed of a series of short but intense peaks typically spanning from 1 to 3 weeks (Fig. 2d). After this period, chl-*a* progressively declined to the levels observed at P1 except on August 2018 when chl-*a* remained high (>1mg m^{-3}) until

September. Additional chlorophyll peaks were observed in October-November, but these are produced by large-scale variations in phytoplankton biomass in the MS produced by water column mixing during autumn in which diatoms are predominant (Basterretxea et al., 2018; Salgado-Hernanz et al., 2022).

Phytoplankton at P1 was typically composed of pico and nanoautotrophs. Conversely, microplankton dominated the assemblages during the outbreaks observed at P2. The most abundant genera were *Gymnodinium, Alexandrium, Heterocapsa, and Prorocentrum* with variable contributions to overall autotrophic microplankton composition (See Fig. 2d). *Gymnodynium* and *Alexadrium* were generally dominant, representing more than 90% of the cells. *Heterocapsa* and eventually *Prorocentrum* were also present although they never accounted for more than 10% of the total cells.

3.3. Characterization of short-term outbreaks

For defining summer blooms at P2, the reference threshold was defined as two standard deviations from the long-term average of the chl-*a* times series at P1 from May to September for the three years and thus estimated at 2.99 mg chl-*a* m^{-3}. Approximately 40 % of the interpolated chl-*a* data at P2 exceeded this threshold during the summer with magnitudes ranging from 3 to 24.92 mg m^{-3} (Fig. 2d and 3). Most (78 %) of the blooms lasted from 10 to 20 days and ranged from 3 to 9 mg chl-*a* m^{-3} (56 % of summer bloom interpolated chl-*a* values, Fig. 3). During the study, 9 summer blooms were registered: 4 in 2017, 2 in 2018 and 3 in 2019. The longest bloom was registered in 2018 lasting 51 days reaching a maximum chl-*a* value of 24.92 mg m^{-3}.

3.4. Plankton metabolism

Gross production in Peguera at P1 was strikingly stable all year round (4.8 ± 0.36 mmol O_2 m^{-3} d^{-1}). Values rarely exceeded 10 mmol O_2 m^{-3} d^{-1} and production per unit biomass yielded 13 ± 99 mmol O_2 mg chl^{-1} d^{-1}). Plankton metabolism at P1 revealed that this coastal ecosystem was close to balance (NCP = -0.85 ± 0.66 mmol O_2 m^{-3} d^{-1}; NCP:CR = -0.05). Differences between P1 and P2 during no-bloom conditions were not significantly different (Friedman test, p >0.01 for GPP, CR, and NCP). Conversely, GPP, NCP, and CR at P2 increased to 5, 12, and 2-fold above P1 reference values in summer (Table 2).

Trends in plankton metabolism at P2 paralleled overall chl-*a* variations, and no evident mismatch was observed between NCP and CR. Instead, a progressive increase in the NCP:CR occurred until August shifting the ecosystem state to autotrophic conditions. This

situation remained until late September when a progressive decline in production and biomass reestablished the balance between production and respiration (Fig. 4d). Remarkably when planktonic metabolism rates are standardized to chl-*a*, NCP differences between P1 and P2 are no longer significant (Friedman test, $p > 0.05$) and seasonal variations of metabolic rates are downsized suggesting that the observed variations during bloom-conditions obey to subtle seasonal changes in metabolism.

4. Discussion

In the present study, we analyzed the year-round variations of phytoplankton biomass and metabolism at a Mediterranean coastal site with recurrent HAB episodes. The studied coastal ecosystem presented outbreaks between May and September, lasting mainly from 10 to 20 days and with mean values of 9.4 mg chl-*a* m^{-3} (maximum values of 25 mg chl-*a* m^{-3}). In the MS, most of the coastal bloom occurred in spring when short-term wind events are more frequent allowing stratification and nutrient supply up to the surface layer and thus, the development of phytoplankton bloom (e.g. Marty et al. 2002). However, HAB events in nearshore ecosystems of the MS occurred mainly in summer and can last for a few days to a month (e.g. Basterretxea et al., 2005; Penna et al., 2005; Vila et al., 2005; Satta et al., 2010). The outbreak dynamics (bloom length and magnitude) at P2 was similar to that reported in the past at the same location (Basterretxea et al. 2005) and in Sicily (Penna et al., 2005; Vila et al., 2005) with intense bloom (chl-*a* > 10 mg m^{-3}) expanding for period of 1-2 weeks. These similarities are mainly explained by a key factor common to each HAB site which is water circulation promoting cell accumulation.

Temperature, salinity, stratification, and nutrients are also long-spotted factors favoring HAB occurrence (i.e. Berdalet et al., 2017, 2014). Consistently with previous studies, the blooming period is well-defined between late May and October when sea surface temperatures exceed 20°C, which seems to be adequate for the growth of local dinoflagellate species. Nevertheless, as shown in Figure 2, the exponential biomass increase was related to increasing temperatures, peaking in August but, even though temperatures remain above this threshold until November, chl-*a* declined and outbreaks became less frequent after the summer temperature maximum. Therefore, consistent with previous studies (e.g. Itakura and Yamaguchi, 2005; Moore et al., 2009), it is suggested that temperature has an impact on the initiation of the bloom and cannot be ruled out that the rising temperatures can stimulate the core metabolism of some HAB-producing dinoflagellates promoting thus the dinoflagellates excystment. For example, temperature-mediated control of dormancy duration has been

reported for the dinoflagellates *Alexandrium catenella* and *Pyrodinium bahamense*—two HAB producing species (Brosnahan et al., 2020).

The role of dormant cysts has been demonstrated to be relevant in shallow high residence time systems where cyst beds are the source of HAB initiation every year (Estrada et al., 2010). The continuous flux of new vegetative cells during the exponential growth phase of the bloom can explain changes in phytoplankton biomass with no alteration of biomass-specific metabolic rates. In the present study, the main phytoplankton genera dominating summer assemblages at P2, *Gymnodinium*, and *Alexandrium*, exhibit life cycles with resting stages. Indeed, Bravo and Anderson (1994) observed that the excystment of *Gymnodinium catanetum* is strongly related to temperature increase with optimal germination and growth of the vegetative population between 22 and 28°C. Likewise, Anderson (1998) observed that the cyst stage is important in *Alexandrium* bloom initiation and termination, particularly in shallow embayments, where cysts and motile cells are tightly coupled. However, despite that cysts production of *Alexandrium* and *Gymnodinuium* genus have been reported along the MS (i.e. Montresor et al., 1998; Bravo et al 2006; Satta et al., 2010), their relative contribution to the early bloom stages in nearshore blooms remains to be quantified.

An additional factor determining the occurrence of nearshore blooms is nutrient availability. Submarine groundwater discharges (SGD) are widespread in Mallorca and a main source of terrestrial nutrients and other elements to the Mediterranean Sea (Basterretxea et al., 2010; Rodellas et al., 2015). Salinity data from Peguera indicates a continuous flux resulting in a nearshore salinity decline. Indeed, salinity at P1 and particularly at P2 showed most of the time values lower than salinity from shelf waters (Fig. 2b). It has been demonstrated that, even in the absence of anthropogenic effects, SGD can effectively stimulate autotrophic plankton growth, thereby producing shifts in the microbial food-web in some cases leading to HABs (Garcés et al., 2011; Gobler and Sañudo-Wilhemy, 2001). Indeed, in meso-environments such as Peguera Beach, nutrient-rich seep from coastal aquifers may sustain high cell abundances of flagellates whose growth would be otherwise limited by the poor nutrient availability prevailing in the MS. However, because of the non-conservative nature of nutrients, their dissolved concentrations do not display good correlations with salinity anomalies (r=0.09, Pearson correlation method). Furthermore, because of the complexity of biotic responses and the influence of other stressors, a signal of changing nutrient concentration does not always elicit a response of changing phytoplankton biomass or production (i.e. Li et al., 2008). Nevertheless, while the canonical relationship between nitrogen and phytoplankton biomass is well established across diverse marine

ecosystems (Smith, 2006), responses depend on community structure. For example, in our case, shoreline nutrient-enriched seeps are mainly capitalized on by large dinoflagellates that can accumulate in large numbers in the nearshore at P2 (up to 10^5 cells l^{-1}). At this site, plankton metabolism rates and, particularly GPP, were mainly driven by the increase in phytoplankton biomass rather than by an enhancement in cell productivity which suggests that nitrogen is aiding to maintain the accumulated cell stock. Indeed, at P2, GPP was significantly correlated with chlorophyll concentration ($r = 0.66$, $P < 0.01$). Additionally, while NCP rates reached a maximum value up to 52 mmol O_2 m^{-3} d^{-1} and showed seasonal variations (Fig. 4), when the rates were corrected per unit of biomass, chlorophyll-specific NCP rates were close to 0 and seasonal variations were not available (data not shown here). These observations suggest that the blooms at P2 are more dependent on accumulation than on sustained growth and production rates.

During the study, the accumulation of planktonic biomass during summer short-term outbreaks at P2 was expected to be related to strong organic matter degradation and thus, to high CR rates. Strong CR rates were indeed observed at P2 during bloom periods reaching a mean value higher than 10 mmol O_2 m^{-3} d^{-1} (Table 2). This mean value was significantly higher than the one observed at P1 at the same period (7.25 mmol O_2 m^{-3} d-1; Table 2) but also higher than the mean values measured in coastal areas of the Balearic Islands (~4 mmol O_2 m^{-3} d^{-1}, Agusti et al., 2017; ~3 mmol O_2 m^{-3} d^{-1}, Gazeau et al., 2005). We can believe thus that the strong respiration of the planktonic community during the summer blooms was highly related to the degradation of organic material. Indeed, microbial respiration can be an important regulator of the C:N of the total organic matter during periods of high productivity such as those encountered during blooms (e.g. Kepkay et al., 1997). However, the higher production compared to respiration (Table 2) indicates a high concentration of particulate organic matter available for transfer to higher trophic levels.

5. Conclusion

In conclusion, the role of enhancement in plankton metabolism on this coastal bloom was weaker than that anticipated by the observed chlorophyll variations. During the summer, the increase in phytoplankton was related to minor chlorophyll-specific NCP variations. The discrepancy between productivity and phytoplankton biomass accumulation could be due to two major factors. First, the contribution of near-shore flow patterns favoring physical cell accumulation at P2. Additionally, benthic excystment could be contributing significantly to cell accumulation and the initial phases of the bloom. Most likely, it is a combination of these

factors that explain chlorophyll trend accumulation and bloom initiation and duration rather than community growth and productivity.

Acknowledgments

This research was financed by HYDROALGAL (RTC-2016-4812-5) project and partially carried out within the framework of the activities of the Spanish Government through the "María de Maeztu Centre of Excellence" accreditation to IMEDEA (CSIC-UIB) (CEX2021-001198-M). A. Regaudie-de-Gioux was supported by a post-doctoral fellowship 'Incorporacion de personal investigador' funded by the Ministry of Innovation, Research and Tourism of the Balearic Island Government. We thank R. Gutierrez and J. Font Munoz for their assistance in the fieldwork and laboratory analyses.

References

Agusti, S., Martinez-Ayala, J., Regaudie-de-Gioux, A., and Duarte, C. M. (2017) Oligotrophication and metabolic slowing-down of a NW Mediterranean coastal ecosystem. *Front. Mar. Sci.*, **4,** 432.

Anderson, D. M. (1998) Physiology and bloom dynamics of toxic Alexandrium species, with emphasis on life cycle transitions. *Nato. Asi. Series G. Ecological Sciences*, **41**, 29–48.

Anderson, D. M., Glibert, P. M., and Burkholder, J. M. (2002). Harmful algal blooms and eutrophication: nutrient sources, composition, and consequences. *Estuaries*, **25**, 704–726.

Basterretxea, G., Font-Muñoz, J. S., Salgado-Hernanz, P. M., Arrieta, J., and Hernández-Carrasco, I. (2018) Patterns of chlorophyll interannual variability in Mediterranean biogeographical regions. *Remote Sens. Environ.*, **215**, 7–17.

Basterretxea, G., Garcés, E., Jordi, A., Anglès, S., and Masó, M. (2007) Modulation of nearshore harmful algal blooms by in situ growth rate and water renewal. *Mar. Ecol. Prog. Ser.*, **352**, 53–65.

Basterretxea, G., Garcés, E., Jordi, A., Masó, M., and Tintoré, J. (2005) Breeze conditions as a favoring mechanism of *Alexandrium taylori* blooms at a Mediterranean beach. *Estuar. Coast. Shelf Sci.*, **62**, 1–12.

Basterretxea, G., Jordi, A., Garcés, E., Anglès, S., and Reñé, A. (2011) Seiches stimulate transient biogeochemical changes in a microtidal coastal ecosystem. . *Mar. Ecol. Prog. Ser.*, **423**, 15–28.

Basterretxea, G., Torres-Serra, F.J., Alacid. E., Anglès, S., Camp, J., Ferrera, I., Flo, E., Font-Muñoz, J.S., et al. (2018) Cross-shore environmental gradients in the Western Mediterranean coast and their influence on nearshore phytoplankton communities. *Front. Mar. Sci.* **5**:78.

Basterretxea, G., Tovar-Sanchez, A., Beck, A. J., Masqué, P., Bokuniewicz, H. J., Coffey, R., Duarte, C. M., Garcia-Orellana, J., et al. (2010) Submarine Groundwater Discharge to the Coastal Environment of a Mediterranean Island (Majorca, Spain): Ecosystem and Biogeochemical Significance. *Ecosystems*, **13**, 629–643.

Beman, J. M., Arrigo, K. R., and Matson, P. A. (2005) Agricultural runoff fuels large phytoplankton blooms in vulnerable areas of the ocean. *Nature*, **434**, 211-214.

Berdalet, E., Fleming, L., Gowen, R., Davidson, K., Hess, P., Backer, L., Enevoldsen, H. (2016) Marine harmful algal blooms, human health and wellbeing: Challenges and opportunities in the 21st century. *Journal of the Marine Biological Association of the United Kingdom*, **96**, 61–91.

Berdalet, E., McManus, M. A., Ross, O. N., Burchard, H., Chavez, F. P., Jaffe, J. S., Jenkinson, I. R., Kudela, R., et al. (2014) Understanding harmful algae in stratified systems: Review of progress and future directions. *Deep Sea Res 2 Top Stud. Oceanogr.*, **101**, 4–20.

Berdalet, E., Montresor, M., Reguera, B., Roy, S., Yamazaki, H., Cembella, A., and Raine, R. (2017) Harmful algal blooms in fjords, coastal embayments, and stratified systems: Recent Progress and Future Research. *Source: Oceanography*, **30**, 46–57.

Bravo, I. and Anderson, D. M. (1994) The effects of temperature, growth medium and darkness on excystment and growth of the toxic dinoflagellate Gymnodinium catenatum from northwest Spain. *J. Plankton Res.*, **16**, 513–525.

Bravo, I., Reguera, B., Martínez, A. and Fraga, S. (1990) First report of *Gymnodinium catenatum* on the Spanish Mediterranean coast. In Graneli, E., Sandstorm, B., Elder, L. and Anderson D.M. (eds.), *Toxic marine phytoplankton*. Elsevier Science, New York, pp. 449–452.

Brosnahan, M. L., Fischer, A. D., Lopez, C. B., Moore, S. K., and Anderson, D. M. (2020) Cyst-forming dinoflagellates in a warming climate. *Harmful Algae*, **91**, 101728.

Calbet, A., Vaqué, D., Felipe, J., Vila, M., Alcaraz, M., and Estrada, M. (2003) Relative grazing impact of microzooplankton and mesozooplankton. *Mar. Ecol. Prog. Ser.*, **259**, 303–309.

Cramer, W., Guiot, J., Fader, M., Garrabou, J., Gattuso, J.-P., Iglesias, A., Lange, M. A., Lionello, P., et al. (2018) Climate change and interconnected risks to sustainable development in the Mediterranean. *Nat. Clim. Chang.*, **8**, 972–980.

Delgado, M., Estrada, M., Camp, J., Fernández, J. V, Santmartí, M., and Lletí, C. (1990) Development of a toxic *Alexandrium minutum* Halim (Dinophyceae) bloom in the harbour of Sant Carles de la Ràpita (Ebro Delta, northwestern Mediterranean).

Donoso, K., Carlotti, F., Pagano, M., Hunt, B. P. V., Escribano, R., and Berline, L. (2017) Zooplankton community response to the winter 2013 deep convection process in the NW Mediterranean Sea. *J. Geophys. Res. Oceans*, **122**, 2319–2338.

Estrada, M., Solé, J., Anglès, S., and Garcés, E. (2010) The role of resting cysts in *Alexandrium minutum* population dynamics. *Deep Sea Res. 2 Top Stud. Oceanogr.*, **57**, 308–321.

Garces, E. (1999) A recurrent and localized dinoflagellate bloom in a Mediterranean beach. *J. Plankton Res.*, **21**, 2373–2391.

Garcés, E., Basterretxea, G., and Tovar-Sánchez, A. (2011) Changes in microbial communities in response to submarine groundwater input. *Mar. Ecol. Prog. Ser.*, **438**, 47–58.

Gazeau, F., Duarte, C. M., Gattuso, J.-P., Barrón, C., Navarro, N., Ruiz, S., Prairie, Y. T., Calleja, M., et al. (2005) Whole-system metabolism and CO_2 fluxes in a Mediterranean

Bay dominated by seagrass beds (Palma Bay, NW Mediterranean). *Biogeosciences*, **2**, 43-60.

Gobler, C. J. (2020) Climate Change and Harmful Algal Blooms: Insights and perspective. *Harmful Algae*, **91**.

Gobler, C. J. , and Sañudo-Wilhemy, S. A. (2001) Temporal variability of groundwater seepage and brown tide blooms in a Long Island embay. *Mar. Ecol. Prog. Ser.*, **217**, 299-309.

Grasshoff, K.. Kremling K, Ehrhardt M. (1999) Methods of seawater analysis, Wiley-VCH, Weinheim, Germany, pp. 159-228.

Irigoien, X., Flynn, K. J., and Harris, R. P. (2005) Phytoplankton blooms: A 'loophole' in microzooplankton grazing impact? *J. Plankton Res.*, **27**, 313–321.

Itakura, S. and Yamaguchi, M. (2005) Morphological and physiological differences between the cysts of Alexandrium catenella and A. tamarense (Dinophyceae) in the Seto Inland Sea, Japan. *Plankton Biology and Ecology*, **52**, 85–91.

Kepkay, P.E., Jellett, J.F. and Niven, S. E. H. (1997) Respiration and the carbon-to-nitrogen ratio of a phytoplankton bloom. *Mar. Ecol. Prog. Ser.*, **150**, 249–261.

Labasque, T., Chaumery, C., Aminot, A., and Kergoat, G. (2004) Spectrophotometric Winkler determination of dissolved oxygen: Re-examination of critical factors and reliability. *Mar. Chem.*, **88**, 53–60.

Lejeusne, C., Chevaldonné, P., Pergent-Martini, C., Boudouresque, C. F., and Pérez, T. (2010) Climate change effects on a miniature ocean: the highly diverse, highly impacted Mediterranean Sea. *Trends Ecol. Evol.*, **25**, 250–260.

Li, W. K. W., Lewis, M. R., and Harrison, W. G. (2008) Multiscalarity of the Nutrient-Chlorophyll Relationship in Coastal Phytoplankton. *Estuaries and Coasts*, **33**, 440–447.

Montresor, M., Zingone, A., and Sarno, D. (1998) Dinoflagellate cyst production at a coastal Mediterranean site. *J. Plankton Res.*, **20**, 2291–2312.

Moore, S. K., Mantua, N. J., Hickey, B. M., and Trainer, V. L. (2009) Recent trends in paralytic shellfish toxins in Puget Sound, relationships to climate, and capacity for prediction of toxic events. *Harmful Algae*, **8**, 463–477.

Padfield, D., Yvon-Durocher, G., Buckling, A., Jennings, S. and Yvon-Durocher, G. (2016) Rapid evolution of metabolic traits explains thermal adaptation in phytoplankton. *Ecol. Lett.*, **19**, 133–142.

Pasqueron de Fommervault, O., Migon, C., D'Ortenzio, F., Ribera d'Alcalà, M., and Coppola, L. (2015) Temporal variability of nutrient concentrations in the northwestern

Mediterranean sea (DYFAMED time-series station). *Deep Sea Res. 1 Oceanogr. Res. Pap.*, **100**, 1–12.

Penna, A., Garcés, E., Vila, M., Giacobbe, M. G., Fraga, S., Lugliè, A., Bravo, I., Bertozzini, E., et al. (2005) *Alexandrium catenella* (Dinophyceae), a toxic ribotype expanding in the NW Mediterranean Sea. *Mar. Biol.*, **148**, 13–23.

Powley, H. R., Krom, M. D., and Van Cappellen, P. (2018) Phosphorus and nitrogen trajectories in the Mediterranean Sea (1950–2030): Diagnosing basin-wide anthropogenic nutrient enrichment. *Prog. Oceanogr.*, **162**, 257–270.

Raven, J. A., and Geider, R. J. (1988) Temperature and algal growth. *New Phytologist*, **110**, 441–461.

Ribera d'Alcalà, M., Conversano, F., Corato, F., Licandro, P., Mangoni, O., Marino, D., Mazzocchi, M. G., Modigh, M., et al. (2004) Seasonal patterns in plankton communities in pluriannual time series at a coastal Mediterranean site (Gulf of Naples): An attempt to discern recurrences and trends. *Sci. Mar.*, **68**, 65–83.

Rodellas, V., Garcia-Orellana, J., Masqué, P., Feldman, M., and Weinstein, Y. (2015) Submarine groundwater discharge as a major source of nutrients to the Mediterranean Sea. *Proceedings of the National Academy of Sciences*, **112**, 3926–3930.

Salgado-Hernanz, P. M., Regaudie-de-Gioux, A., Antoine, D., and Basterretxea, G. (2022) Pelagic primary production in the coastal Mediterranean Sea: variability, trends, and contribution to basin-scale budgets. *Biogeosciences*, **19**, 47–69.

Satta, T. C., Anglès, S., Garcés, E., Lugliè, A., Mario Padedda, B., and Sechi, N. (2010) Dinoflagellate cysts in recent sediments from two semi-enclosed areas of the Western Mediterranean Sea subject to high human impact. *Deep Sea Res. 2 Top Stud. Oceanogr.*, **57**, 256–267.

Smith, V. H. (2006) Smith, Val H. Responses of estuarine and coastal marine phytoplankton to nitrogen and phosphorus enrichment. *Limnol. Oceanogr*, **51**, 377–384.

Stolte W., and Garces E. (2006) Ecological aspects of harmful algal in situ population growth rates. In Granéli, E.and Turner, J.T. (eds.) *Ecology of Harmful Algae*. Ecological Studies, Vol. 189 Springer-Verlag Berlin Heidelberg, pp. 139-152.

Vila, M., Giacobbe, M. G., Masó, M., Gangemi, E., Penna, A., Sampedro, N., Azzaro, F., Camp, J., et al. (2005) A comparative study on recurrent blooms of *Alexandrium minutum* in two Mediterranean coastal areas. *Harmful Algae*, **4**, 673–695.

Ward, B. A., Marañón, E., Sauterey, B., Rault, J., and Claessen, D. (2017) The size dependence of phytoplankton growth rates : A trade-off between nutrient uptake and metabolism. *American Naturalist*, **189**, 170-177.

Wells, M. L., Karlson, B., Wulff, A., Kudela, R., Trick, C., Asnaghi, V., Berdalet, E., Cochlan, W., et al. (2020) Future HAB science: Directions and challenges in a changing climate. *Harmful Algae*, **91**.

Wells, M. L., Trainer, V. L., Smayda, T. J., Karlson, B. S. O., Trick, C. G., Kudela, R. M., Ishikawa, A., Bernard, S., et al. (2015) Harmful algal blooms and climate change: Learning from the past and present to forecast the future. *Harmful Algae*, **49**, 68–93.

Table and Figure legends

Table 1. Mean ± SE, minimum, maximum, and number of observations (*N*) of sea surface temperature, salinity, NOx concentration, and chl-*a* during the sampling period of this study at P1 and P2.

Table 2. Measured mean ± SE of volumetric metabolism rates (NCP, CR, and GPP; mmol O_2 m^{-3} d^{-1}) and chl-*a* concentration (mg m^{-3}) during bloom (May-September) and non-bloom conditions (October-April) at P1 and P2.

Figure 1. Map of Peguera Beach in the west coast of Majorca (Balearic Islands) and location of the two sampling points (P1 and P2).

Figure 2. Temporal variation of sea surface temperature (a), salinity (b), NOx concentration (error=22% of mean value) (c), and chl-*a* concentration (d) at P1 (white dots) and P2 (black dots). Vertical grey-shaded areas indicate bloom periods. (a) Blue and red lines represent the sinusoidal function adjustment to P1 and P2 discrete samples, respectively. (b) Salinity at P1 and P2 and reference offshore salinity at Palma Bay (blue line, https://www.socib.es/?seccion=observingFacilities&facility=mooring&id=143).(d) Chl-*a* (mean ±std) is shown in a logarithmic scale. The exponential phase in biomass (chl-*a*) build-up is indicated by dashed blue lines and the green dashed line indicates the reference threshold, sad described in Section 2.4. Pies on top of (d) indicate the average microplankton community composition during each bloom period.

Figure 3. Frequency distribution and its corresponding percentage of chl-*a* range and the length of the short-term outbreaks at P2 during bloom periods (May-September).

Figure 4. Temporal variation of CR (a), GPP (b), NCP (c) and GPP:CR ratios (d) at P1 and at P2 during the sampling period of the study . Vertical grey-shaded areas indicate bloom periods. The low-pass filtered signal of the GPP:CR ratios are shown to reveal the seasonality in P1 (blue) and P2 (red).

Tables

Table 1.

		Mean ± SE	min	max	N
Temperature (°C)	**P1**	22.32 ± 0.39	14.1	29.07	147
	P2	23.28 ± 0.43	14.1	30.8	148
Salinity	**P1**	37.36 ± 0.03	36.3	38.1	146
	P2	37.23 ± 0.04	34.9	38.2	147
NOx concentration ($mmol\ m^{-3}$)	**P1**	0.80 ± 0.04	0.1	3.51	141
	P2	1.06 ± 0.06	0.1	5.61	143
chl-*a* ($mg\ m^{-3}$)	**P1**	0.45 ± 0.09	0.11	12.75	147
	P2	2.97 ± 0.40	0.15	24.92	148

Table 2.

	Non-Bloom				Bloom			
	chl-*a*	**NCP**	**CR**	**GPP**	**chl-*a***	**NCP**	**CR**	**GPP**
P1	0.41 ± 0.04*	0.21 ± 1.30	6.31 ± 0.72	5.47 ± 0.83	0.47 ± 0.12*	-1.33 ± 0.75*	7.25 ± 0.64*	4.61 ± 0.37*
P2	0.71 ± 0.12*	-1.26 ± 1.51	7.05 ± 0.77	5.42 ± 0.88	3.99 ± 0.54*	10.68 ± 2.09*	13.32 ± 0.98*	24.82 ± 2.33*

*variables significantly different between P1 and P2 for each period (Friedman test, $p < 0.05$)

Figures

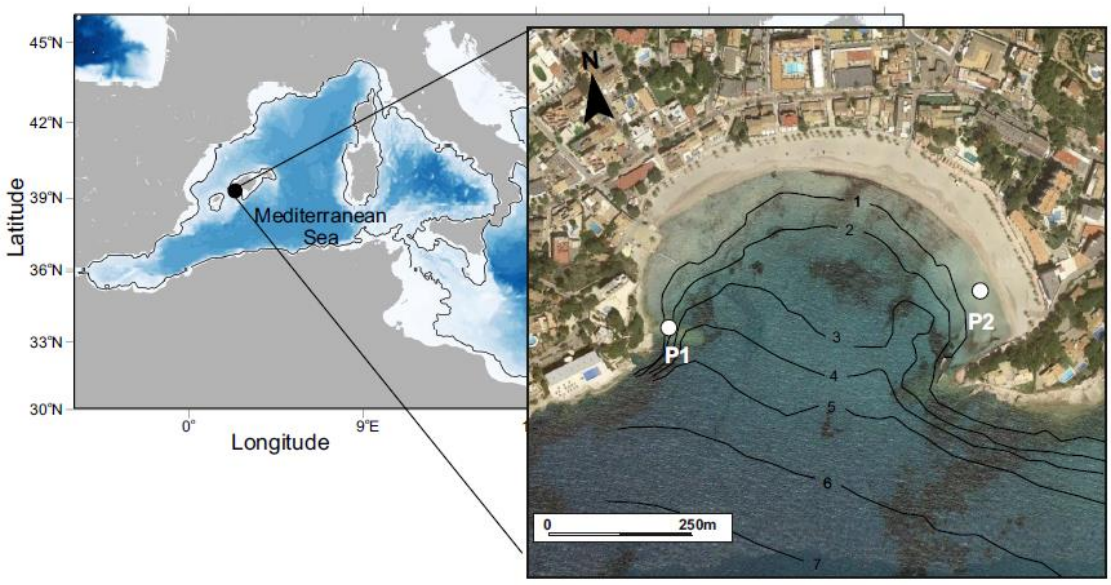

Figure 1.

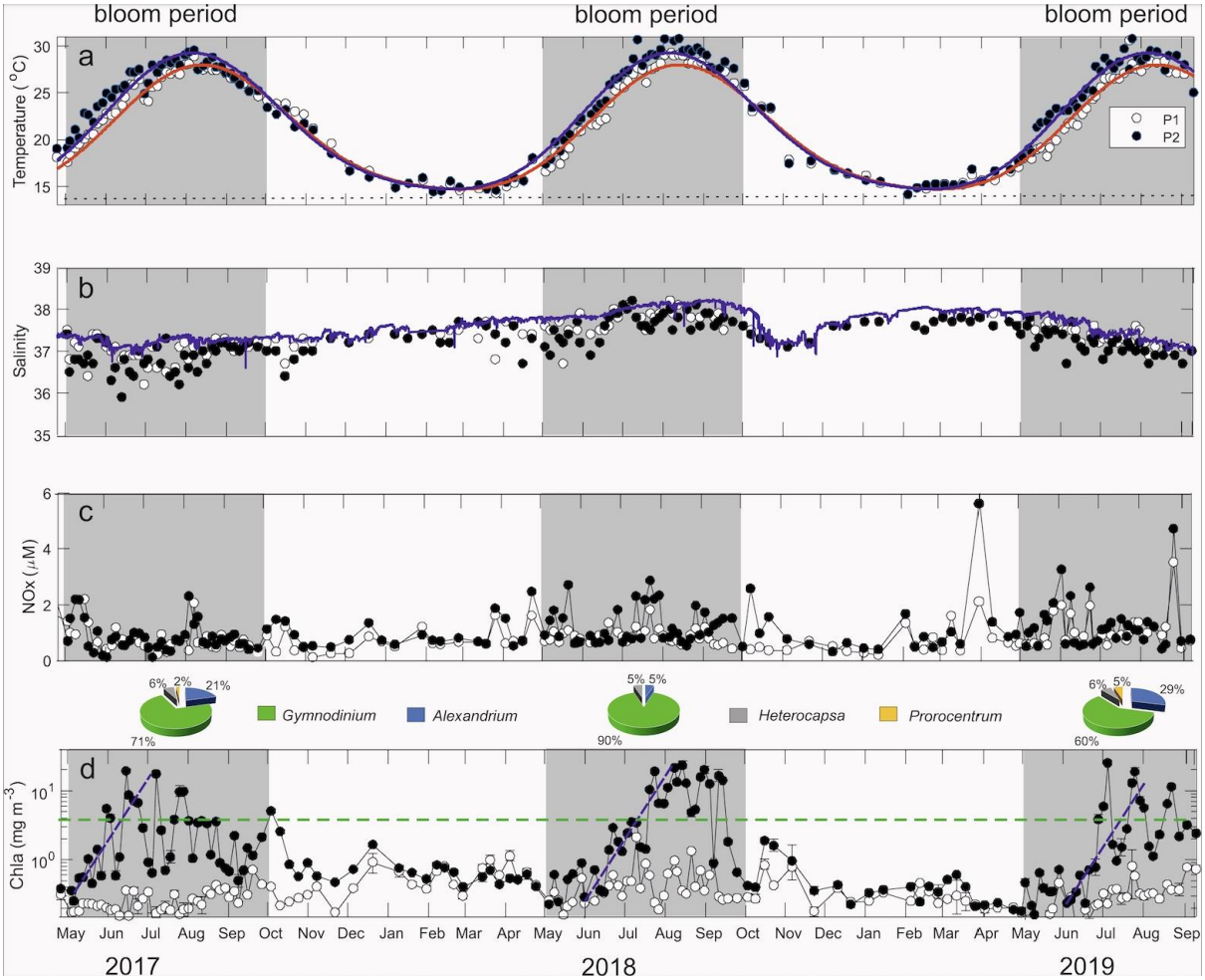

Figure 2.

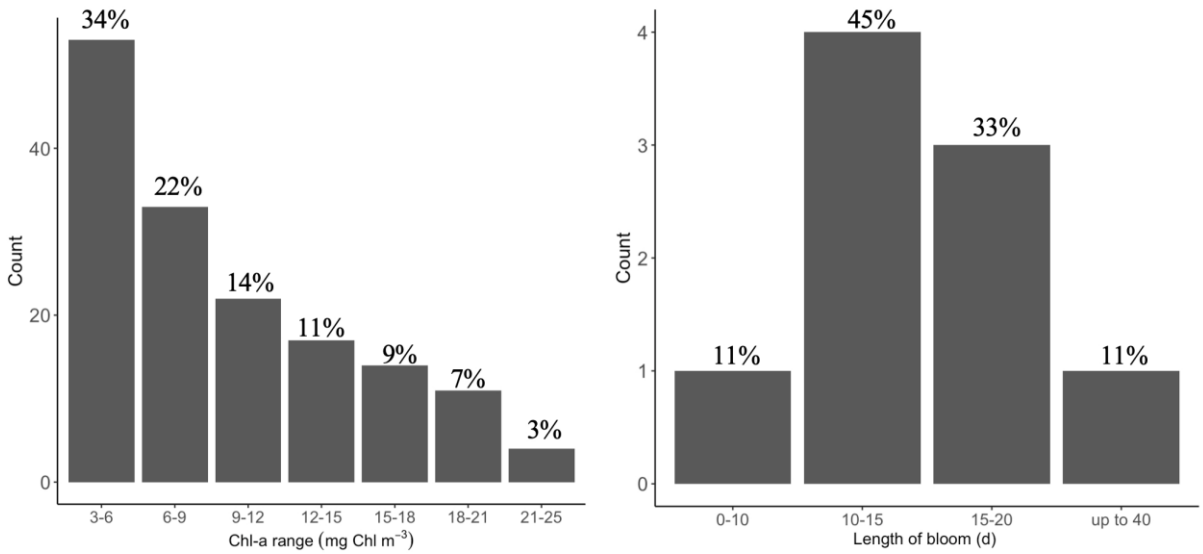

Figure 3.

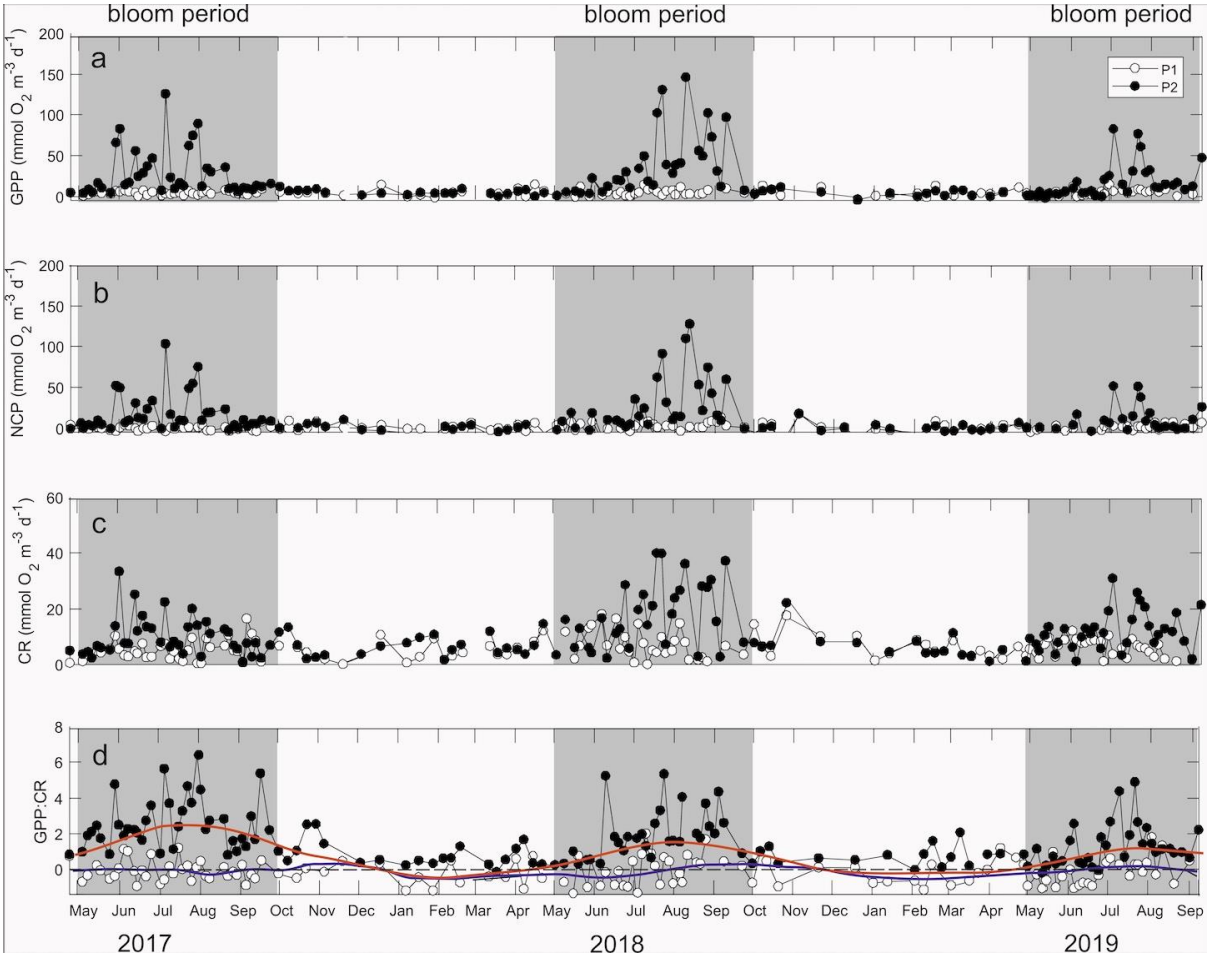
bloom period
bloom period
bloom period
a
b
c
d
P1
P2
GPP (mmol O2 m-3 d-1)
NCP (mmol O2 m-3 d-1)
CR (mmol O2 m-3 d-1)
GPP:CR
May Jun Jul Aug Sep Oct Nov Dec Jan Feb Mar Apr May Jun Jul Aug Sep Oct Nov Dec Jan Feb Mar Apr May Jun Jul Aug Sep
2017
2018
2019

Figure 4.